Capillary force in atomic force microscopy

Joonkyung Jang, George C. Schatz, and Mark A. Ratner

Citation: The Journal of Chemical Physics **120**, 1157 (2004);
View online: https://doi.org/10.1063/1.1640332
View Table of Contents: http://aip.scitation.org/toc/jcp/120/3
Published by the American Institute of Physics

Capillary force in atomic force microscopy

Joonkyung Jang
School of Nano Science and Technology, Pusan National University, Geomjeong-gu, Busan 609-735, South Korea

George C. Schatz and Mark A. Ratner
Department of Chemistry, Materials Research Center and Center for Nanofabrication and Molecular Self Assembly, Northwestern University, Evanston, Illinois 60208-3113

(Received 7 August 2003; accepted 17 November 2003)

Under ambient conditions, a water meniscus generally forms between a nanoscale atomic force microscope tip and a hydrophilic surface. Using a lattice gas model for water and thermodynamic integration methods, we calculate the capillary force due to the water meniscus for both hydrophobic and hydrophilic tips at various humidities. As humidity rises, the pull-off force rapidly reaches a plateau value for a hydrophobic tip but monotonically increases for a weakly hydrophilic tip. For a strongly hydrophilic tip, the force increases at low humidities ($<30\%$) and then decreases. We show that mean-field density functional theory reproduces the simulated pull-off force very well.
 [DOI: 10.1063/1.1640332]

The interaction between an AFM tip (typically with a sub-100 nm radius) and a surface is fundamentally changed by the water meniscus that naturally forms between them in air. The recently developed dip-pen nanolithography,[1] for example, utilizes the meniscus as a channel for diffusion of molecules from the tip to a substrate. A more general effect of the meniscus is the capillary force that usually governs the force on the AFM tip.[2] This force (and therefore image) changes substantially as we vary humidity[3–5] and the hydrophilicity of the tip.[5,6] Unfortunately, transparent interpretation of these experiments is hampered by various unknown factors[3] such as the tip geometry, surface corrugation, and contamination. It is thus difficult to conclude whether the pull-off force on a mica surface should be monotonically increasing[3] or nonmonotonic[4] as humidity increases.

Theoretical investigation provides an avenue for removing experimental uncertainties and providing clear insights into the capillary force. One approach to determining force is the macroscopic Laplace–Kelvin equation.[7] However, for nanoscale problems, this approach is not appropriate because of finite molecular size effects that give large fluctuations in meniscus size and shape. Also, the macroscopic approach incorrectly assumes that the meniscus shape can be described by two principal radii, and its volume remains unchanged as the tip is retracted. Molecular theories,[8] including molecular dynamics and Monte Carlo simulations, integral equation and density functional theories, therefore provide an attractive alternative. Previously, we studied the capillary force by using a Monte Carlo simulation based on a two-dimensional lattice gas model.[9] This demonstrated how thermodynamic integration methods can be used to calculate the force in a lattice model of the system. Here, we study fundamental issues concerning capillary forces and meniscus structure by considering a spherical AFM tip in three dimensions interacting with a planar substrate (see Fig. 1). For this prototypical geometry, we systematically study the effect of humidity and molecule-tip interaction strength on capillary force. We also propose a mean-field DFT[10] approach as a computationally effective method for calculating the pull-off force.

Our simulations refer to a cubic lattice with lattice spacing l, wherein molecules are confined between a spherical tip and a plane substrate. Each molecule interacts with its nearest neighbor molecules with an attractive energy ϵ and has its own chemical potential μ. It binds to the tip and substrate surfaces (if it is located right next to the surfaces) with energies b_T and b_S, respectively. Simulations are run by using the isomorphism of the lattice gas model to an Ising model.[11] Only the first quadrant of the system $(x,y \geqslant 0)$ is updated by Monte Carlo steps, and the rest of the system is constructed by taking mirror images of the first quadrant with respect to the XZ plane, YZ plane, and the Z axis. No molecules are allowed to exist outside the horizontal boundaries of our system $(x,y=30l)$. Simulation with this system leads to nearly identical results to those obtained without invoking reflection symmetry, or with periodic boundary conditions.

The bulk critical temperature for the lattice gas is given by $k_B T_c/\epsilon = 1.128$. Identifying our liquid as water ($T_c = 647.3$ K) sets $\epsilon = 4.771$ kJ mol^{-1}. The temperature is fixed at $T/T_c = 0.46$, corresponding to water at room temperature. If we further use the typical lattice spacing $l = 0.37$ nm for the lattice gas model of water,[12] our force unit is $\epsilon/l = 0.021$ nN. The substrate is modeled after gold, which is a common substrate in dip-pen nanolithography.[1] From ab-initio calculations of the water-gold attraction (29.7 kJ mol^{-1}) (Ref. 13) and hydrogen bond strength (18.63 kJ mol^{-1}) (Ref. 14) we take $b_S/\epsilon = 1.594$. With this binding energy, the substrate is completely wet[15] by liquid in our model, and it thus may be considered strongly hydrophilic. As in our previous work,[9,16] we consider three different tip binding energies: a *strongly hydrophilic* tip with the same binding energy as that of the substrate, a *weakly hydrophilic* tip having $b_T/\epsilon = 0.75$ which is partially wet[15] by the liquid, and a *hydrophobic* tip with $b_T/\epsilon = 0.2$ (a value suggested for a hydrophobic surface[17]). For the above energetic parameters

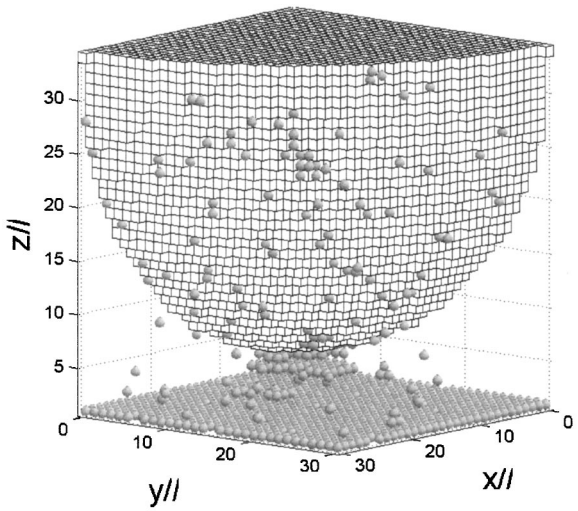

FIG. 1. System geometry and a representative configuration of liquid (drawn as spheres). At relative humidity 30%, a liquid meniscus has condensed between a weakly hydrophilic AFM tip (drawn as cubes) and a plane substrate (located at $z=0$). The spherical tip has a radius of 30 lattice spacings (l). If we use a typical lattice spacing for water ($l=0.37$ nm[12]), the radius is roughly 11 nm. Shown is the 1st quadrant of the system, $0 \leqslant x, y \leqslant 30l$.

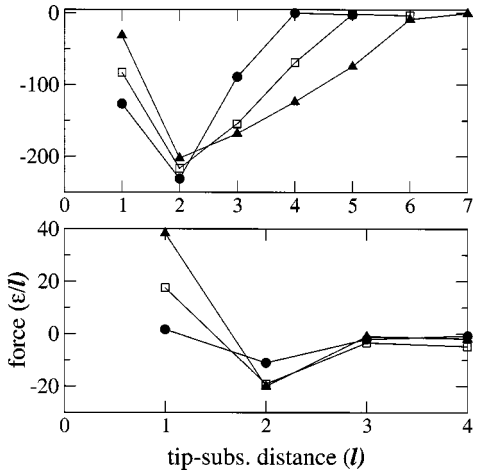

FIG. 2. The capillary force vs the tip-substrate distance. The distance unit is the lattice spacing l, and the force unit is ϵ/l (ϵ=molecular attraction energy). For the strongly hydrophilic (top) and the hydrophobic (bottom) tips, the force-distance curve is evaluated at relative humidities of 30% (filled circles), 50% (open squares), and 70% (filled triangles). The force is attractive (repulsive) if it is negative (positive). In this and all the following figures, lines are drawn as a visual guide.

and temperature, we ran simulations by varying the tip-substrate distance and humidity. We define *relative humidity* (RH) as $\mathrm{RH}=\exp[(\mu-\mu_c)/\mathrm{k_B T}]$, where μ_c is the chemical potential at the bulk gas–liquid transition ($=-3\epsilon$).[18]

In Fig. 1, we show a snapshot of the liquid meniscus formed between the weakly hydrophilic tip and the strongly hydrophilic substrate at RH 30%. Note that the weakly hydrophilic tip is partially covered by molecules but the strongly hydrophilic substrate is completely covered (wet) by liquid. In terms of the contact angle between the liquid–vapor and liquid–solid surfaces, the meniscus has roughly 90° and 0° contact angles with the tip and the substrate, respectively. Note that a meniscus in our definition always includes a monolayer on the substrate. We will show later that the monolayer is responsible for a constant force with respect to humidity change for the hydrophobic tip. By averaging over many (40 000) snapshots such as in Fig. 1, we calculate the average occupancy of each site in our system. The resulting density profile is cylindrically symmetric and is used for the force calculation in the DFT (see below).

We calculate the capillary force by using thermodynamic integration methods previously described.[9] These methods assume that a thermodynamic equilibrium is maintained during the approach or retraction of the tip. The dynamic or inertial effects due to the loading rate of the AFM tip are thus missing. Briefly, the capillary force F(h) is given by[19]

$$\mathrm{F(h)}=-\left(\frac{\partial\Omega}{\partial \mathrm{h}}\right)_{\mu,T}-p\left(\frac{\partial V}{\partial \mathrm{h}}\right)_{\mu,T}, \tag{1}$$

where Ω is the grand potential of the system, h is the tip-substrate distance, V is the system volume, and p is the pressure of the bulk system. In the *T integration* method, we utilize the following relation,[20]

$$\left.\frac{\partial(\beta\Omega)}{\partial\beta}\right|_{\mu,h}=\mathrm{E}-\mu\mathrm{N} \quad (\beta^{-1}=\mathrm{k_B}T), \tag{2}$$

where E and N are energy and number of molecules in the system, respectively. We integrated Eq. (2) numerically by carrying out a series of simulations starting from a very high temperature (where the exact Ω is known). Taking the numerical derivative of Ω obtained this way, we can calculate the force given by Eq. (1). In the μ *integration* technique, we use,[21]

$$\left(\frac{\partial \mathrm{F}}{\partial\mu}\right)_{h,T}=\left(\frac{\partial \mathrm{N_{ex}}}{\partial \mathrm{h}}\right)_{\mu}, \tag{3}$$

where $\mathrm{N_{ex}}$ is the excess number of molecules relative to that in bulk. Starting from a sufficiently low chemical potential (which gives zero force), we run simulations by gradually increasing the chemical potential up to a desired value with numerical integration of Eq. (3).

The force-distance curve calculated by using the T integration method is shown in Fig. 2. With increasing humidity, the force becomes longer ranged (diminishes at a longer distance) for the hydrophilic tip. In contrast, the force for the hydrophobic tip effectively vanishes above a tip-substrate distance of $2l$, regardless of humidity. The vanishing force is due to evaporation of the meniscus as the tip retracts from the substrate. For the hydrophilic tip, the menisci have concave shapes and disappear at a longer tip-substrate distance as humidity rises. For the hydrophobic tip, however, the only meniscus that forms regardless of humidity is a monolayer of molecules sandwiched between the tip and the substrate (and the corresponding tip-substrate distance is $2l$). Thus the force becomes zero when the tip-substrate distance is longer than $2l$. Also note in the figure that, when the tip is in contact with the substrate (tip-substrate distance$=l$), the force is still attractive for the hydrophilic tip, but for the hydrophobic tip it is repulsive. This can be explained as follows. At the

contact distance, the tip actually squeezes a monolayer of molecules (approximately 97 molecules) out of the area where the tip contacts with the flat substrate. For the hydrophilic tip, the system can compensate this loss of a monolayer by forming a bigger meniscus. That is, as the system gets more confined (due to the closer tip-substrate distance), molecules at the interface feel stronger interaction with the tip and substrate and thus form a bigger meniscus. As a result, the system is more stable (smaller Ω) when the tip is in contact with the substrate and therefore the force is attractive. For the hydrophobic tip however, bringing the tip in contact with the substrate removes a portion of a monolayer from the substrate surface. Because of the weak molecule-tip attraction, the geometric confinement at the contact does not yield a bigger meniscus as with the hydrophilic tip. Therefore, this change is energetically unfavorable and thus gives a repulsive force. It should be noted that our calculation deals with the capillary force only. The total force, which includes the van der Waals force, will be repulsive at the contact even for a hydrophilic tip. Regardless of tip hydrophilicity and humidity, the force is most attractive at the closest noncontact distance ($2l$). For the hydrophilic tip, the dip in the force curve at the closest noncontact distance ($2l$) broadens and decreases in depth as humidity goes up. In contrast, the dip at the same distance for the hydrophobic tip gets deeper as humidity rises from 30% to 50% and stays the same as humidity further increases to 70%. The magnitude of this maximum attractive force is called the *pull-off force*, and we will examine its behavior with respect to humidity later.

Running a succession of simulations required for the thermodynamic integration is computationally intensive even after parallelizing our codes (we have to deal with up to ~26 700 molecules). As a computationally efficient alternative to our simulation, we have tested a density functional theory (DFT) approach. DFT has played a leading role in the study of phase behavior of confined fluids. It has been used (but not tested) to calculate the capillary force in a surface force apparatus experiment[22] whose geometry is similar to a slit. Here, we apply mean-field DFT[10] to our system. The grand potential Ω_{DFT} in the DFT[10] is given by

$$\Omega_{\mathrm{DFT}}=\sum_i \left[\rho_i \log \rho_i+(1-\rho_i)\log(1-\rho_i)\right] - \frac{\epsilon}{2}\sum_{\substack{i,j=\\ \text{nearest}\\ \text{neighbors}}} \rho_i\rho_j+\sum_i (V_i-\mu)\rho_i , \qquad (4)$$

where ρ_i is the average occupancy of the ith site, and V_i is the surface field (both from the tip and substrate) at the ith site. We used the density profile ρ_i from our Monte Carlo simulation as the input in Eq. (4) to calculate Ω_{DFT}. We then calculated the force by using Eq. (1).

In Fig. 3, the force from the DFT is compared to that from the T integration method. DFT compares well with the simulation at a low humidity (40%) [top]. At a high humidity (80%) [bottom], it fails to predict the sign of the force at the contact distance (l). At a tip-substrate distance of $4l$, there is a huge discrepancy between the DFT and simulation. This distance is right before the water meniscus snaps off (evaporates). This deficiency of DFT at the snap-off distance is found at RH=70, 80% for hydrophilic tips. Otherwise, DFT accurately duplicates the simulated forces at short distances including the pull-off forces (see below). We interpret the above shortcoming of DFT as follows. At high humidities for the hydrophilic tips, the meniscus becomes large in size. Snap-off of the meniscus thus resembles a bulk liquid–gas phase transition, where long-ranged density correlation is important. The DFT, which considers only local density fluctuations, fails to capture the long-range phenomena.

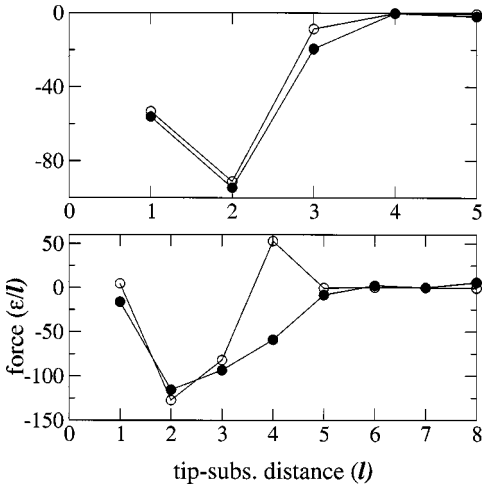

FIG. 3. Capillary force calculated from DFT. For a weakly hydrophilic tip, the DFT force (○) is compared to that (●) from the thermodynamic integration method. Relative humidities are 40% (top) and 80% (bottom).

Finally, we plot in Fig. 4 the pull-off force as a function of humidity for tips with different hydrophilicities. The DFT

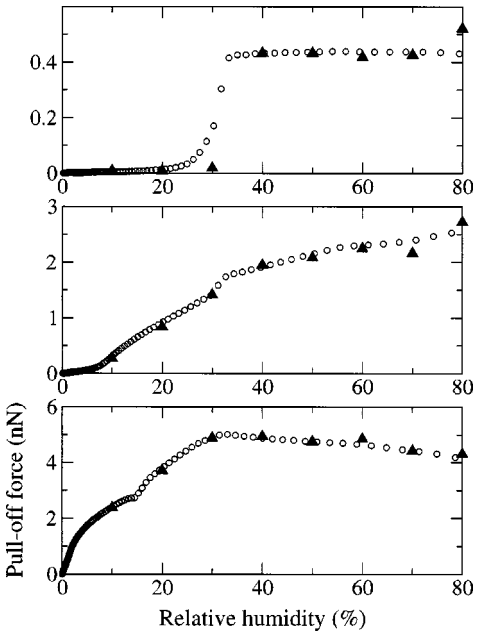

FIG. 4. Humidity dependence of the pull-off force for different tip hydrophilicities. The forces calculated from the μ integration method (open circles) and density functional theory (triangles) are plotted for the hydrophobic (top), weakly hydrophilic (middle) and strongly hydrophilic tips (bottom). The force is converted to physical dimensions relevant to water at room temperature (see text).

result compares very well with both the μ integration and T integration methods (the latter not shown). The average pull-off forces (at humidities 10–80%) are roughly 0.3, 1.7, and 3.9 nN for the hydrophobic, weakly hydrophilic, and strongly hydrophilic tips, respectively.

Our simple model reproduces the magnitude of the pull-off force typically found in experiment (several nN).[3–5] Depending on tip hydrophilicity, we see a distinct humidity dependence to the pull-off force. For the hydrophobic tip, the force is zero up to 20% humidity because there is no water meniscus between the tip and the substrate. The force then increases rapidly and reaches a plateau value at around 30% humidity. As mentioned previously, the meniscus for the hydrophobic tip corresponds to a monolayer confined between the tip and the substrate. This monolayer is mainly due to the hydrophilic substrate and, once formed at humidity 34%, stays nearly uniform as humidity goes up. Therefore, the pull-off force remains constant at humidities above 34%. Experimentally, a constant behavior of pull-off force with respect to humidity change has been reported for a hydrophobic tip on a silicon surface.[5] When the tip is made weakly hydrophilic, the pull-off force becomes appreciable already at RH of 10% and steadily rises with humidity increase. For the strongly hydrophilic tip, the force is nonzero at humidities as low as 1%, and the force is now a nonmonotonic function of humidity. It increases with humidity up to 30%, and then gradually decreases with humidity increase. Both monotonic increase[3] and nonmonotonic behavior (similar to our calculation)[4] of the force with respect to humidity rise have been observed experimentally.

We have shown that some features of the capillary force can be understood by delving into the details of water meniscus structure. Using a well defined geometry that emulates an AFM tip, we could unambiguously address the effect of the tip hydrophilicity on the pull-off force. A hydrophobic tip feels a constant pull-off force at humidities above a certain value due to a water monolayer formed on the substrate surface. If the tip is weakly hydrophilic, the force increases monotonically with humidity. For a strongly hydrophilic tip, the force increases and then decreases as humidity increases. We also found that the mean field DFT is almost quantitative in predicting the pull off forces.

ACKNOWLEDGMENTS

This research was supported by AFOSR MURI Grant F49620-00-1-0283 and by the National Science Foundation. We thank Chad Mirkin for helpful discussions.

[1] R. D. Piner *et al.*, Science **283**, 661 (1999); S. Hong and C. A. Mirkin, *ibid.* **288**, 1808 (2000).
[2] J. Israelachvili, *Intermolecular and Surface Forces* 2nd Ed. (Academic, London, 1992).
[3] D. L. Sedin and K. L. Rowlen, Anal. Chem. **72**, 2183 (2000).
[4] L. Xu *et al.*, J. Phys. Chem. B **102**, 540 (1998).
[5] M. He *et al.*, J. Chem. Phys. **114**, 1355 (2001).
[6] T. Eastman and D. Zhu, Langmuir **12**, 2859 (1996).
[7] T. Stifter, O. Marti, and B. Bhushan, Phys. Rev. B **62**, 13667 (2000).
[8] For reviews, see L. D. Gelb *et al.*, Rep. Prog. Phys. **62**, 1573 (1999).
[9] J. Jang, G. C. Schatz, and M. A. Ratner, Phys. Rev. Lett. **90**, 156104 (2003).
[10] M. J. De Oliveira and R. B. Griffiths, Surf. Sci. **71**, 687 (1978).
[11] K. Binder and D. Stauffer, in *Applications of the Monte Carlo Method in Statistical Physics*, edited by K. Binder (Springer, Berlin, 1987). 2nd ed.
[12] L. Maibaum and D. Chandler, J. Phys. Chem. B **107**, 1189 (2003).
[13] A. Ignaczak and J. A. N. F. Gomes, J. Electroanal. Chem. **420**, 209 (1997).
[14] S. J. Grabowski, Chin. Phys. Lett. **338**, 361 (2001).
[15] R. Pandit, M. Schick, and M. Wortis, Phys. Rev. B **26**, 5112 (1982).
[16] J. Jang, G. C. Schatz, and M. A. Ratner, J. Chem. Phys. **116**, 3875 (2002).
[17] A. Luzar and K. Leung, J. Chem. Phys. **113**, 5836 (2000).
[18] T. L. Hill, *Statistical Mechanics* (McGraw-Hill, New York, 1956), Chap. 7.
[19] R. Evans and U. Marini Bettolo Marconi, J. Chem. Phys. **86**, 7138 (1987).
[20] B. K. Peterson and K. E. Gubbins, Mol. Phys. **62**, 215 (1987).
[21] S. G. Ash, D. H. Everett, and C. Radke, Faraday Trans. II **69**, 1256 (1973).
[22] L. J. Douglas Frink and F. van Swol, J. Chem. Phys. **106**, 3782 (1997).